CONF-880506--29

WHC-SA-0205-FP

Fast Flux Test Facility Passive Safety Reactivity Feedback Measurements

B. J. Knutson
R. A. Harris
D. H. Nguyen
R. P. Omberg

WHC-SA--0205

DE89 011857

Date Published
March 1988

Presented at the
American Nuclear Society Topical Meeting
on the Safety of Next Generation
Power Reactors
Seattle, Washington
May 1-5, 1988

Prepared for the U.S. Department of Energy
Assistant Secretary for Nuclear Energy

Westinghouse Hanford Company
P.O. Box 1970
Richland, Washington 99352

Hanford Operations and Engineering Contractor for the
U.S. Department of Energy under Contract DE-AC06-87RL10930

FAST FLUX TEST FACILITY PASSIVE SAFETY REACTIVITY FEEDBACK MEASUREMENTS

B. J. Knutson, R. A. Harris, D. H. Nguyen, and R. P. Omberg

Westinghouse Hanford Company
P. O. Box 1970 (MSIN L7-25)
Richland, WA 99352

ABSTRACT

A series of experiments conducted in the Fast Flux Test Facility (FFTF) measured the reactivity change between approximately 200 reactor states. The test data have been evaluated to determine the thermal hydraulic parameters of the reactor at those states. Auxiliary measurements have been analyzed to convert the measured control rod position changes to reactivity and to correct for burnup effects. The data are now available for studies of the temperature reactivity feedbacks in liquid metal reactors. Preliminary comparisons with a feedback algorithm developed from normal FFTF operation indicate that the functional form of feedbacks can be extrapolated to offnormal conditions.

INTRODUCTION

During February and March of 1986, an extensive series of steady state reactivity feedback experiments was conducted at the Fast Flux Test Facility (FFTF). These tests were part of a national effort to develop a passively safe reactor design that can accommodate a large range of accident conditions without relying on special engineered safety components or continuous electrical power to operate coolant pumps. The primary goal of the tests was to determine the magnitude and source of temperature reactivity feedback effects existing in the reactor. This information can then be used to verify the computer models that will be used to predict the reactivity feedbacks in new designs.

This paper provides the rationale used in designing the tests, the techniques and criteria used to evaluate the data and their uncertainties, and finally provides a comparison with a feedback model developed for FFTF.

TEST DESIGN

A. General

The objective of the test series was to identify and quantify the reactivity feedbacks in FFTF through a series of measurements of the reactivity change between a variety of reactor states. The basis for the tests is the assumption that the dependence of known feedback effects on changes in reactor temperatures is reasonably well known. For example, the feedbacks from uniform radial expansion are directly proportional to the magnitude of increases in the coolant inlet temperature. The magnitude of the feedbacks is not as well known.

Using the assumed temperature dependence of the feedbacks, reactor state changes were developed to emphasize or deemphasize each of the known feedback mechanisms. In some cases an individual feedback or groups of feedbacks could be isolated, i.e., all others eliminated, and the magnitude of the feedback(s) could be measured directly. For example, if the power level is changed and the flow rate is modified to maintain the coolant temperatures, only the temperatures inside the fuel pins will change. The observed reactivity change can then be attributed to the fuel material alone. This isolation is not possible for most of the feedbacks. Their magnitudes can be determined in a least squares technique, however, using all of the state-change data if the relative magnitudes of the feedbacks vary in the data.

The tests were divided into four series, or sequences, of measurements. Each sequence contained approximately 50 similar reactor maneuvers; however, each was initiated from a different power level and power-to-flow ratio. Overall, the reactor power was varied between 10% and 100% while coolant conditions ranged from 67% to 100% flow rate and 303 °C (577 °F) to 360 °C (680 °F) core inlet temperature. These parameter ranges were dictated by constraints on allowable operational conditions.

B. Experimental Constraints

The primary sodium coolant flow rate was maintained within the range of 67% to 100% of full flow. Operation at flow rates below 67% would interfere with a plant protection system

(PPS) low-flow trip and could produce excessive resonant vibrations in the pumps at rates near 61%. Also, the safety analyses for FFTF did not address extended plant operation under such conditions.

The limits on the secondary loop cold leg temperatures for this test program were <338 °C (640 °F) and >293 °C (560 °F). No important plant limits would be violated if these limits were exceeded slightly; however, this restriction permitted the use of the automatic secondary cold leg temperature controllers and greatly simplified the operator actions.

There is an operational limit that the vertical position of any two of the six control rods may not differ by more than 2.5 in. During these tests the reactor was maneuvered between each of the states using only control rod no. 8. This permitted a more accurate interpretation of the reactivity change. Periodically the control rod bank was repositioned so that control rod no. 8 would not exceed the position limit on subsequent state changes.

C. Test Descriptions

A description of the seven reactor state-change types used to isolate, eliminate, emphasize, or deemphasize individual feedbacks is described in test Types 1 through 7.

Test Type 1. Fuel Effects. The reactor inlet and outlet temperatures are held constant while the reactor power and coolant flow rate are varied, keeping the power-to-flow ratio constant.

To first order, the temperatures of the coolant and structural materials in the reactor do not change in this measurement. Any reactivity effect observed must then be the result of changes in the fuel material temperatures.

Test Type 2. Structural Effects, Constant Average Coolant Temperature. The average temperature of the fuel pin columns is held constant by keeping both the reactor power level and axially averaged coolant temperature constant while the flow rate is increased. The change in power-to-flow ratio is accommodated by increasing the core coolant inlet temperature.

This test generates feedbacks from all structural feedback components in the reactor because both inlet and outlet temperatures change. Holding the average coolant temperature constant tends to reduce the contribution from uniform radial expansion of the core. The large change in the temperature drop across the core, however, enhances the contribution from assembly bowing.

Test Type 3. Structural Effects, Constant Outlet Coolant Temperature. This measurement is very similar to test Type 2 because an attempt is made to eliminate any fuel feedbacks. As the flow rate is increased, the core outlet temperature is held constant by increasing the inlet temperature. Some change in reactor power is necessary to maintain the fuel temperatures constant because the average coolant temperature increases.

As in test Type 2, only structural feedbacks are observed. Holding the core outlet temperature constant eliminates expansion of the control rod driveline and any radial expansion at the top of the core. Bowing certainly contributes but the expansion effect of the core support plate is the dominant feedback.

Test Type 4. Temperature Coefficient. The temperature of the coolant entering the reactor core is varied in this measurement while holding the reactor power level and flow rate constant.

All components in the reactor experience a uniform temperature increase. The major feedbacks come from uniform radial expansion. The contribution from assembly bowing is small because the temperature gradients across the ducts remain nearly constant. There may be some changes in the gaps at the load planes, however, and this could cause a small bowing effect. The fuel effects are small because the fuel temperatures are most sensitive to changes in reactor power.

Test Type 5. Flow Coefficient. The flow rate of the coolant entering the reactor core is varied in this measurement while holding the reactor power level and coolant inlet temperature constant.

The major reactivity feedbacks in this test come from assembly bowing because the power-to-flow ratio changes dramatically. There are contributions from all components except the core support plate.

Test Type 6. Controlled Transient. This measurement statically simulates a transient in which the coolant flow rate is reduced without any control rod movement. The reactor power is allowed to seek a new level to compensate for the reactivity change caused by the increase in coolant temperatures. This compensation is obtained by changing the fuel temperatures.

All feedback components contribute in this measurement. However, the sign of the fuel feedbacks is opposite that of most of the other components because they are compensating. This test is a small-scale example of the feedback effects that will occur in a loss-of-flow incident.

Test Type 7. Power Coefficient. The power level is changed in this measurement

while holding the coolant inlet temperature and flow rate constant. The dominating feedbacks come from the fuel temperature changes.

D. Test Matrix

The primary data for achieving the test objectives are obtained in test Types 1, 2, 3, 4, and 6. The flow and power coefficient data (Types 5 and 7) offer another view of the total reactivity feedbacks and, therefore, enhance the data base. They, along with the temperature coefficient data (Type 4), also serve an additional function. They provide data which can be used to correct the primary data for small deviations from the desired reactor conditions. For example, it may be determined in later analyses that a different reactor power level was required to eliminate the fuel feedbacks from the Type 2 structural effects measurement. The power coefficient measured at the end of test Type 2 will provide the needed accurate reactivity correction.

E. Data Collection Method

Special computer codes were used to collect data on magnetic tape and to provide real-time display of the reactor state conditions to the reactor operators. Upon request, during steady-state conditions, the power and primary flow indications were calibrated to the thermal power and flow rates inferred from a heat balance on the secondary coolant loops. The displayed parameters included both filtered (i.e., averaged) and unfiltered quantities.

The reactor variables recorded on tape included the individual primary and secondary loop, hot and cold leg temperatures and flow rate sensors as well as the neutron channel indications. Data from the approximately 2000 variables monitored by the standard plant data collection system are also available. The reactor operators manually recorded detailed control rod position indications at each equilibrium state.

F. Measurement Method

Zero power differential rod worth measurements were performed to accurately characterize the worth of the test rod in its movement about a fixed bank position. At-power test rod worths were measured at the main test states using Multi-Frequency Binary Sequence (MFBS) tests to allow accurate conversion of the test rod position movements to reactivity at power conditions.

Transition between the test states was made by moving control rod no. 8 together with changes in reactor parameters such as primary and secondary pump flow rates or heat rejection to ambient through the dump heat exchangers. The reactor operators controlled the reactor changes during test state transitions by monitoring the special computer displays as well as the normal plant instrumentation. The transitions were made in smooth progression while maintaining parameters designated as constant from state to state within tolerance ranges so as not to create additional transients. Having both filtered and unfiltered parameters displayed was especially helpful in this regard.

Once equilibrium reactor conditions were established, after no external reactor condition changes (e.g., rod movements, flow rate adjustments, etc.) by the operators for 15 min, the 6-min calibration routine was started within the data collection program. The revised calibration factors were then applied to the nuclear power and primary flow sensor values that were being displayed to the reactor operators.

If the power, flow, and temperature values fell outside specified tolerance ranges, changes were made to the reactor. Any changes dictated another 15 min waiting period without operator manipulations of the reactor state. The tolerances were slightly larger than the statistical fluctuations of the filtered values of the reactor parameters.

DATA EVALUATION

A. Test State Identification

Equilibrium test state periods were located on the data records using plots of the main reactor variables. Whenever there was a delay in starting a new state-change measurement, equilibrium periods immediately following the previous transient and just before the next transition were identified.

A data processing code then made a fit to the important reactor test variables to determine the mean values and possible trends over the equilibrium periods. Statistically significant trends were detected for nearly all reactor parameters. However, they were small and were not important for the purposes of these tests.

B. Calibration Algorithms

The algorithms used to provide a thermal power calibration and to scale the primary flow rate meters are standard equations used to monitor the performance of the plant during normal operation. They are especially important for this report because they are the most significant source of uncertainty in the data.

The primary algorithm extracts the thermal power (Q) from a heat balance applied to the secondary coolant loops and has the form

$$Q = \sum_{i=1}^{3} (Q_i + Q_L - Q_{Pi})$$

where

Q_i = thermal power transferred to secondary loop i
Q_L = power lost through piping
Q_{Pi} = power from primary pump work.

The thermal power Q_i for each secondary loop i is determined from the expression

$$Q_i = F_{Si} \int_{T_{CS,i}}^{T_{HS,i}} C_p(T)\, dT$$

where

$T_{CS,i}$ = secondary cold leg temperature
$T_{HS,i}$ = secondary hot leg temperature
F_{Si} = secondary mass flow rate
$\int C_p(T)\, dT$ = coolant enthalpy change.

The heat loss (Q_L) is small and has a value of 0.08%/loop, or a total of 0.25% of full thermal power.

The heat added by the primary pump work (Q_P) is also small (~1%) and is based on the flow rate and the pressure drop across each pump.

The primary flow rate was determined by assuming the heat losses in the intermediate heat exchangers are negligible and that each secondary loop power is equal to each primary loop power, or

$$Q_{PRI} = Q_{SEC} \text{ or,}$$

$$F_{Pi} \int_{T_{CP,i}}^{T_{HP,i}} C_p(T)\, dT = F_{Si} \int_{T_{CS,i}}^{T_{HS,i}} C_p(T)\, dT$$

where P denotes the primary loops.

C. Control Rod Worths

The reactivity worth of movements of the control rods (RHO) in FFTF has traditionally been computed from an algorithm of the form

$$RHO = W_T \sum_{i=1}^{6} R_i \sum_{j=1}^{5} X_1^j\, a_j$$

where

W_T = total worth of the rod bank
X_1 = position of the i^{th} rod
R_1 = relative worth of rod i
a_j = rod bank profile coefficients.

This form is used because the six rods used to control FFTF are always operated in a nearly banked configuration. The profile coefficients refer to the entire bank rather than to individual rods. These coefficients were developed from data collected during the first seven cycles of operation. The data included zero power measurements at the end of each cycle where up to 22 in. of the bank could be measured. Also, the rate of rod withdrawal during full power operation was used to improve the profile. Experience has shown that the profile has not changed noticeably from cycle to cycle.

The calibration used for this series of tests consisted of measuring the reactivity worth of movements of each control rod ± 2 in. from the rod bank at zero power during startup. The technique used was the Modified Source Multiplication (MSM) method of inferring reactivity from count rate changes in a slightly subcritical reactor.[1] The data included measurements at 0, +1, +2, -1, -2, and 0 in. from the bank position. These were fit to the profile in a least squares functional to determine the differential worth (cents /inch) of each rod. The measurements yielded the relative rod worths (R_i) shown in Table 1. The total worth of moving the bank the same ± 2 in. was determined by summing the measured worth of each rod. The parameter W_T was adjusted so that the algorithm yielded this total worth. The value obtained for W_T was 1725.9 ± 7.7 ¢.

Table 1. Measured Relative Rod Worths

Rod No. (i)	Relative Rod Worths (R_i)
4	0.992 ±0.008[a]
5	0.962 ±0.015
6	1.004 ±0.007
7	1.075 ±0.005
8	0.958 ±0.016
9	1.009 ±0.010

[a]Uncertainties are one standard deviation.

D. Burnup Corrections

During the conduct of the feedback tests, significant burnup reactivity losses occurred. These were most pronounced, of course, when the reactor power level was highest. Corrections to remove these effects initially were obtained by computing the losses from the detailed power history during the tests using the standard FFTF operational monitoring algorithm. This algorithm includes both the burnup of fissile isotopes and the decay of ^{239}Np to ^{239}Pu.

After the feedback tests were completed the reactor was operated at full power for 35 days. The deviation, anomaly, between the measured rod positions and those predicted from the burnup algorithm and pretest estimates

of the rod bank worth is shown in Figure 1. Over this period of operation, the burnup reactivity loss was predicted to be -10.90 cents/day. The data were fit to a straight line. From the slope of the fit it was found that the control rods were being withdrawn 6.7 ± 0.5% slower than predicted. The computed burnup reactivity losses were then scaled down by 6.7%.

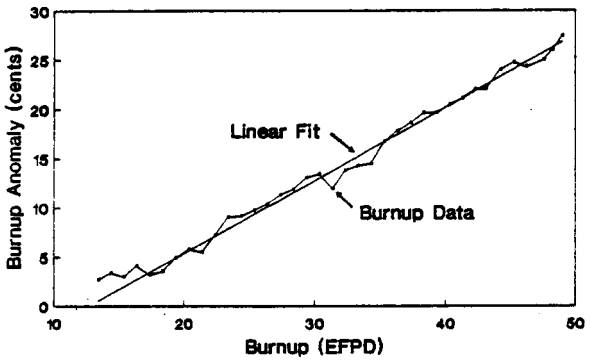

Figure 1. Burnup Reactivity Loss Data

This procedure provides corrections consistent with the rod worths predicted before startup. The rod calibration measurements indicated that the early predictions were too large. The burnup corrections were then further scaled down to be consistent with the rod worths to be used in the analysis of the data.

UNCERTAINTIES

A. Thermal Hydraulic Parameters

The uncertainties in the thermal hydraulic parameters extracted from the data records are the result of the statistical uncertainties in the parameters used to enter the calibration algorithms and possible biases in the sensors themselves. The impact of the statistical uncertainties was determined by first noting that, to first order, uncertainties in conduction heat loss and pump work terms can be neglected. Reactivity feedbacks are sensitive only to changes in power in units of per cent of full power (MW). Even a 10% error in these terms would yield a power uncertainty of only 0.13% which is insignificant. Therefore, the dependence of the primary plant variables on measured quantities can be approximated by

$$Q \propto F_S * (T_{HS} - T_{CS})$$

$$F_P \propto Q / (T_{HP} - T_{CP})$$

where the i subscript has been dropped.

The statistical uncertainties in the measured variables can then be propagated through to Q and F_P using standard techniques and assuming all measurements are independent. The results of such calculations, applied to three different test states and averaged over all loops, are shown in Table 2. The dramatic increase in the uncertainty in F_P as the power drops is the result of the lower temperature drops across the secondary and primary loops. This increases the effect of uncertainties in the hot and cold leg temperatures. This is not a significant limitation in the data, however, because no reactivity feedbacks occur directly from a change in flow rate. Instead they depend on the temperature changes induced by the flow rate change. These are characterized by a change in the power-to-flow ratio. As seen in Table 2, the uncertainty in this ratio is small (0.19 to 0.14% of the full-power ratio). This is because both Q and F_P depend directly on F_S and the secondary loop temperature drops and, thus, are strongly correlated. A measure of this correlation is given by the term ρ_{Q,F_P} in the table. This quantity is the ratio of the "covariance" of Q and F_P divided by the standard deviation of each quantity. Values near one indicate strong correlation.

Table 2. Sample Statistical Uncertainties

	States 1	2	3
Conditions			
Power (Q, %)	95.0	10.1	9.4
Flow (F_p, %)	100.0	66.81	100.7
Inlet (T_{CP}, °C)	359.9	338.7	338.4
Statistics			
σQ [a]	0.51	0.18	0.25
σF_P	0.57	1.37	3.06
σT_{CP}	0.23	0.21	0.20
$\sigma Q/F_P * 100$	0.19	0.16	0.14
ρ_{Q,F_P} [b]	0.94	0.86	0.86
$\rho_{F_P,T_{CP}}$	0.30	0.48	0.48

[a] σX = one standard deviation (X = variable)
[b] $\rho_{A,B}$ = correlation coefficient $= \sigma^2_{A,B} / (\sigma_A \sigma_B)$

The uncertainty in Q is seen to decrease as the power level drops. The relative uncertainty ($\sigma Q/Q$) increases over these tests but reactivity feedbacks are most sensitive to the magnitude of power changes (in units of per cent of full power).

There is some correlation in the uncertainties in F_P and T_{CP}. However, it is not dramatic as evidenced by the correlation coefficients of 0.30 to 0.48.

The data contains additional uncertainty due to the inaccuracies in the installed plant

sensors. The estimated one standard deviation error due to the possible biases in all of the instruments required for a thermal power assessment near full power is 2.1% (of full power). This uncertainty obviously must be considered in the final analysis of the data, however, its impact may not be large. The reactivity measurements all involve changes in reactor state. The instrument inaccuracies should be directly correlated at the two states and therefore should contribute little error.

B. Control Rod Worths

The uncertainties in the control rod reactivity changes are the result of uncertainties in the zero power calibration of the reactivity algorithm and the extrapolation of that calibration to the bank positions of the test. These are shown in Table 3. The calibration component comes from the measurements of the small rod movement worths, the worth of the rod bank and the calibration of the MSM[1] technique. It is largely the result of neutron counting statistics.

Table 3. Rod Movement Reactivity Uncertainties

Source	Rods Moved: Bank	Rods Moved: Rod 8
Zero power calibration	0.9%[a]	1.8%
Extrapolation to test states	1.0%	1.0%
Total	1.4%	2.1%

[a]Uncertainties are one standard deviation.

The uncertainty in extrapolating the zero power calibration to the bank positions of the tests can only be approximated. Figure 2 indicates how the differential worth (cents/inch) of the control rod bank varies with bank position.

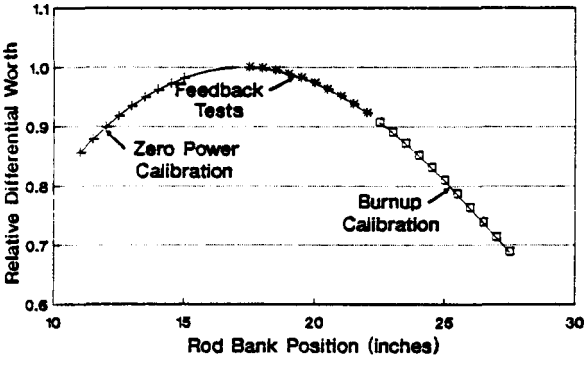

Figure 2. Differential Rod Worth Ranges

During the calibration process, the relative differential worth varied from 0.86 to 0.98. At the mean bank position of the calibrations (~13 in.) the value is 0.94. During the feedback tests the mean relative worth was ~0.96, or very similar to that at the calibration state. Obviously, if these relative worths are accurate, there would be little uncertainty introduced by extrapolating the calibration data. The only possible mechanism identified which could affect these worths is a shift in the peak of the curve in Figure 2. A full 0.5 in. shift would be required to alter the relative differential worth at the test conditions by 1%. For this report it will be assumed that such a shift is possible and a conservative uncertainty of $\pm$ 1% (1σ) was assigned. It should be noted that there is very little uncertainty in the position of the control rods. The FFTF uses stepping motors to position the rods and the movements can be determined very accurately from the activated phases of the motors.

The basic shape of the differential worth curve was also confirmed by reviewing the rate of withdrawal of the rod bank to compensate for burnup reactivity losses. These results, discussed in the following section, cover yet a third area of the curve.

The final, or total uncertainties are shown in Table 3 for both rod bank movements and for movements of control rod no. 8. These uncertainties apply only to scaling factors (W_T and R_I) and, therefore, are correlated for sequential reactivity changes. In other words, they should be applied to reactivity differences. For example, the uncertainty in the reactivity change between two reactor states in which only control rod no. 8 was moved is 2.1% of the change. The uncertainties in changes spanning several test types become more complicated since there may be some bank movements also. This can be conservatively simplified by using the control rod no. 8 uncertainties for all changes. The Table 3 uncertainties are the only ones to be applied to the rod movement data since, as discussed previously, it is assumed that there is no rod position uncertainty.

C. Burnup Corrections

The scaling of the burnup reactivity corrections by 6.7% introduces an uncertainty of 0.5%. Extrapolation of the burnup calibration data to the rod bank positions of the feedback tests will add additional uncertainty. From Figure 2 it can be seen that this extrapolation involves an ~20% increase in differential rod worth. However, it is expected that this increase can be relatively well predicted. During the burnup calibration the rod bank was moved from 22.5 to 27.5 in. withdrawn. This covers a range of differential rod worths which differ by 32%. This change was well predicted as evidenced by the quite linear behavior of the anomaly in Figure 1. Based on this obser-

vation, extrapolation of the burnup calibration data is estimated to add an uncertainty of 2%.

No uncertainty is added by scaling the burnup results to reflect the measured rod bank worths. This is because the burnup calibration was actually in terms of inches on the rod bank and not reactivity.

The final, total uncertainty on the burnup corrections is the quadratic combination of 0.5% and 2% since these uncertainties are independent of each other. The resulting quantity, 2.1%, is correlated for each reactor state and, therefore, should be applied to differences as for the control rod reactivity uncertainties.

DATA ANALYSIS

It is not possible to provide tabulations of the evaluated data in this paper; however, it is expected that a public document with this data will be available in 1988. The reactivity changes over each test sequence are shown in Figures 3 through 6. The general trends in the data were evaluated by comparing them with a feedback prediction model developed for FFTF operation. This is shown as the "Predicted-Measured" curves on the figures. The model was originally based on theoretical predictions of the feedback effects known to exist in FFTF. It was then adjusted to force agreement with the control rod position data recorded during normal startup and shutdown. These operations cover only a limited range of inlet temperature and only full flow rates. A limited amount of data was obtained at 75% flow during acceptance testing of the reactor and factored in along with power and inlet temperature coefficient data. The final form of the model represents the total feedback effects and not the individual components.

The agreement is quite good for the highest power sequence (Figure 3). Agreement near full power was expected because most of the data used to construct the model were generated at such conditions. Most of the states from steps 15-40, however, were at ~60% power with abnormally low flow rates and coolant inlet temperatures. This indicates that the temperature dependence retained in the model from its theoretical origins is basically correct.

The agreement gets progressively worse as the power levels decrease (Figures 4, 5 and 6). This is expected because there was not a lot of data in this region used in constructing the model. A preliminary analysis indicates that the characteristic shape of the difference curve is strongly correlated with the lowest power-to-flow ratio states in each sequence. That is, the model overpredicts the reactivity changes associated with going to a low power, high flow rate state.

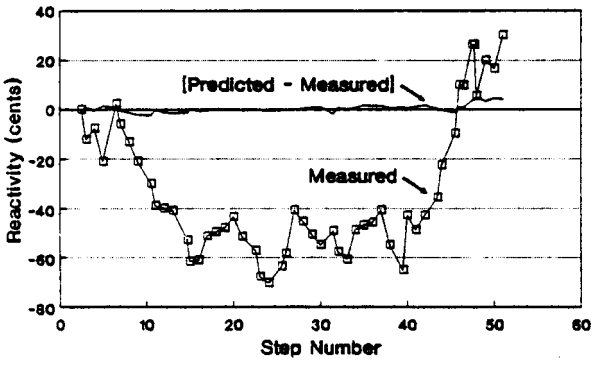

Figure 3. Sequence 1 Data (59 to 96% Power)

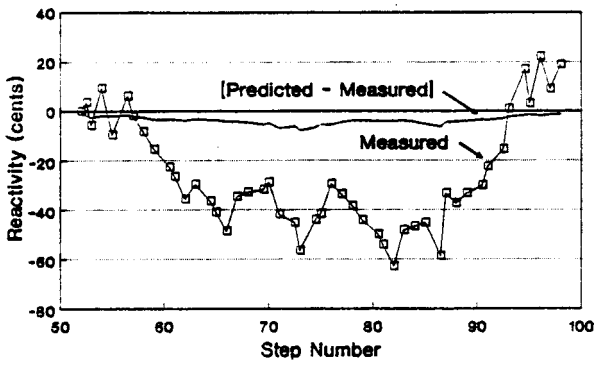

Figure 4. Sequence 2 Data (35 to 60% Power)

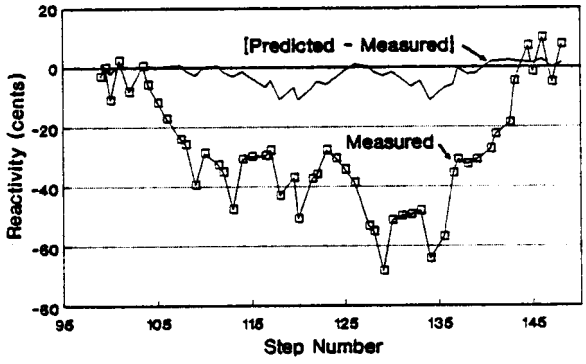

Figure 5. Sequence 3 Data (24 to 36% Power)

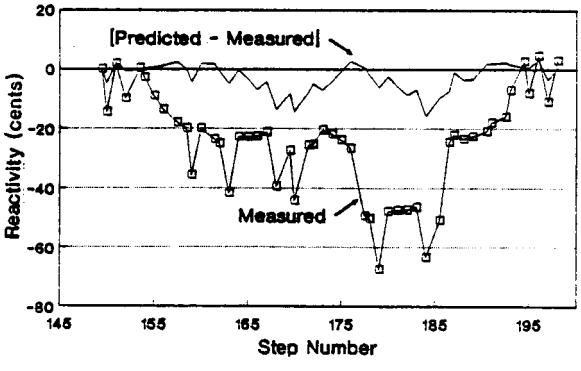

Figure 6. Sequence 4 Data (10 to 22% Power)

In general the data appear to be reasonable and the analyses to extract the individual feedback mechanisms should proceed. It should be noted that the FFTF model, confirmed by this data, is not in agreement with theoretical models. In particular, the model yields a much larger inlet temperature reactivity coefficient than was predicted for FFTF.

CONCLUSIONS

The analysis of the data to separate the individual reactivity feedbacks and, thus, evaluate prediction models has not been completed. However, an evaluation of the data and their uncertainties indicates that they are consistent with the test objectives.

For instance, the ~0.5% uncertainty on reactor power level will have a negligible effect on extraction of fuel feedback effects from the data. This is because the fuel feedback tests (Type 1) involve large power and reactivity changes. The reactivity changes in the structural feedback tests (Types 2 and 3), however, were much smaller. In these tests, the temperature and, thus, reactivity changes were driven mostly by changes in the power-to-flow ratio which is known quite well (see Table 2). Therefore, it should be possible to extract both types of feedback effects (fuel and nonfuel) from the data.

The reactivity calibration of the control rods to <2.1% is more than adequate to characterize the reactivity changes. This uncertainty is applied to changes only and will be exceeded by those of the reactor parameters in most instances. This relatively small uncertainty was obtained because the test program was designed so that the control rods would be near the peak worth condition ($\pm$ 6 in. of 18 in. withdrawn) for both the calibration of the rods and the performance of the PS tests.

The burnup reactivity loss calibration data resulted in corrections to the feedback data which were accurate to 2.1%. There is no identified need for smaller uncertainties in these corrections.

REFERENCE

1. P. A. OMBRELLARO et al., "Evaluation of MSM for Assessing Subcritical Reactivities in FFTF," Trans. Am. Nucl. Soc., 35, 526 (1980).

DISTRIBUTION

Number of Copies

Onsite

BCS Richland, Inc.

2 Central Files, L8-04

3 Document Clearance Coordinator, L8-15

1 Documentation, L8-15

2 Publication Services, L8-07

U. S. Department of Energy
Richland Operations Office

5 M. S. Karol, A5-35

Westinghouse Hanford Company

1 R. A. Bennett, N2-32

1 J. W. Daughtry, L7-25

2 R. A. Harris, L7-25

2 B. J. Knutson, N2-32

2 D. H. Nguyen, L7-26

2 R. P. Omberg, L5-59